TRANSIENT TEMPERATURE RISE AT SURFACE DUE TO ARBITRARY CONTACTS ON HALF-SPACES

K.J. NEGUS and M.M. YOVANOVICH

Microelectronics Heat Transfer Laboratory
Department of Mechanical Engineering,
University of Waterloo
Waterloo, Ontario, Canada, N2L-3G1

Received January, 1987. Revised Manuscript Received June 10, 1987.
No. 87-CSME-06. EIC Accession No. 2135

Approximate analytical methods have been developed to predict the transient temperature rise at surface points interior or exterior to arbitrarily-shaped contacts with uniform heat flux on a homogeneous half-space. The solution for points interior to the contact is based on subdivision into triangular surface elements. For points exterior an approximate solution is derived by integrating across a contact of arbitrary shape. The resultant expressions are easily implemented on a microcomputer and can be used to describe the transient thermal behaviour of large systems of contacts.

Augmentation transitoire de la température d'une surface causee par des contacts arbitraires en demi-espace

Des méthodes analytiques approximatives ont été développées pour prédire l'augmentation transitoire de la température d'une surface en présence de contacts de forme arbitraire avec flux de chaleur uniforme d'un demi-espace homogène. Pour des points internes aux contacts, la solution est basée sur une subdivision en éléments triangulaires. Pour des points externes aux contacts, une solution approximative est obtenue en intégrant sur le contact de forme arbitraire. Les expressions obtenues peuvent être appliquées à l'aide d'un microordinateur et servent à décrire le comportement thermique transitoire de systèmes à plusieurs contacts.

NOMENCLATURE

- a - sector radius; ellipse semi-major axis; radius of a circle
- A - contact area
- A_e - area difference caused by macro-discretization
- b - obtuse triangle side length; ellipse semi-minor axis; sector radius
- c - obtuse triangle side length
- Fo - Fourier modulus or dimensionless time - used in several contexts
- G_{ij} - matrix relating contact fluxes to contact temperatures at a given time
- I_o - polar second moment of area about centroid of the j^{th} contact area
- I_{RR} - radial second moment of area about axis through centroid of j^{th} contact area and point P
- k - thermal conductivity
- L - chord length
- n - number of triangular macro-elements
- P - point at which temperature rise is calculated
- q - uniform flux on contact
- r - polar coordinate
- R - distance between centroid of j^{th} contact and point P
- t - time
- T - temperature rise
- T^* - dimensionless temperature rise

Greek Symbols

- α - thermal diffusivity
- β - dimensionless distance from centroid of contact
- δ - length of perpendicular of right-triangle
- ϵ - error in T^*
- θ - polar coordinate
- ρ - distance from point source
- ω - vertex angle of triangle; vertex angle of sector

Subscripts and Superscripts

- i - denotes i^{th} contact
- j - denotes j^{th} contact
- l - denotes l^{th} triangular macro-surface element

INTRODUCTION

To accurately predict the electrical performance of modern semiconductor devices in integrated circuits, the transient thermal behaviour of the devices is often required. A common modelling assumption for this problem is that each device can be treated as a discrete, uniformly-heated, planar thermal contact on the surface of the semiconductor die. A silicon or gallium arsenide die is typically 200-300 μm in thickness and 1000 μm or more in length and width. However, the characteristic dimension of an individual device or thermal contact is only several μm and thus for times on the order of device transients (nanoseconds) the planar heat sources behave essentially as contacts on a homogeneous half-space. In addition, convective and radiative heat transfer from the surface is usually negligible compared to conduction into a copper or beryllium oxide heat sink attached to the base of the die. The resultant thermal problem for this application is thus one of determining the transient thermal behaviour of a large system of arbitrary planar contacts on the surface of an adiabatic half-space as shown in Figs. 1 and 2. Note that although arbitrarily-shaped contacts are shown in Fig. 1, common shapes such as rectangles or ellipses are usually encountered in practical applications. Furthermore, to study the transient thermal behaviour for heating which varies over times on the order of seconds (for example, initial power-up) a more comprehensive model which accounts for the layered structure of complete system must be developed.

Solution methods presently available for solving three-dimensional transient heat conduction problems include the finite element method and the finite volume and finite difference methods. However, a modern semiconductor die can easily have many hundreds of active planar thermal contacts and thus an extremely large computational effort may be required to analyze these dies using conventional numerical methods. For the special case where a system of contacts on a half-space is allowed to reach steady-state, an efficient approximate solution method, the surface element method, has recently been developed [1]. In this work the surface element method is

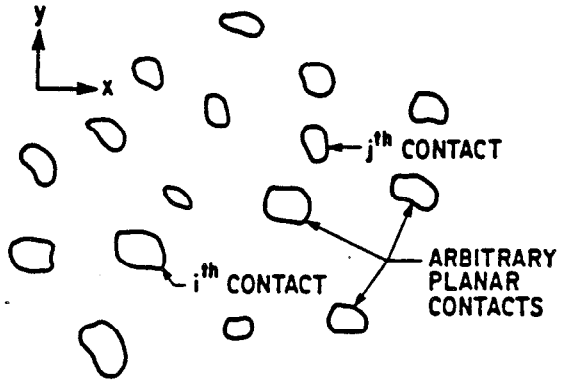

Fig. 1 Arbitrary planar contacts on adiabatic half-space (plan view)

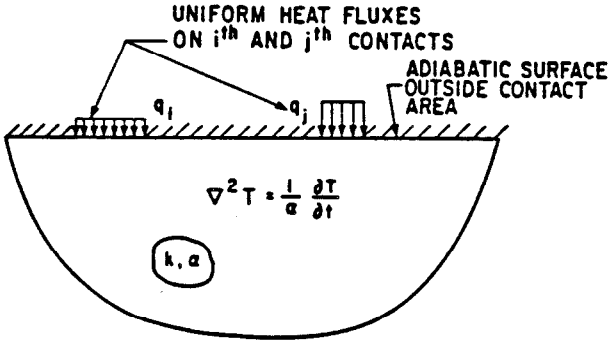

Fig. 2 Arbitrary Planar contacts on adiabatic half-space (section view)

extended to predict the transient temperature rise of large systems of planar contacts.

The computational efficiency of the surface element method derives directly from the use of linear superposition principles for heat-flux specified contacts on an adiabatic half-space. The temperature, T_i, at some interior point of the i^{th} contact in Figs. 1 or 2 is written conceptually as

$$T_i = T_{ii} + \Sigma T_{ij} \qquad (1)$$

In this form T_{ii}, the self-effect, represents the transient temperature rise due to the i^{th} contact acting alone on an adiabatic half-space. Each T_{ij}, the induced-effect, represents the transient influence at a point exterior to the j^{th} contact also acting alone on an adiabatic half-space. The summation in Eq. (1) is assumed to be taken over all contacts in the system.

The surface element formulation has two major advantages in terms of computational simplicity. First, the self-effect and induced-effect components can be treated separately using approximately analytical techniques to derive simple expressions. Second, the results obtained, usually the centroidal contact temperatures, are exactly the information required for subsequent device analysis. That is, large amounts of computer time are not expended to predict unneeded temperatures at every point in space and time as with the fully numerical approaches.

In this work the self-effect component T_{ii} is determined for arbitrary shapes by super-position of triangular elements. The induced-effect component T_{ij} is derived for arbitrary shapes approximately but accurately at least for "long time" conditions. Although possible to determine, it is shown that the "short term" condition for T_{ij} usually has little practical significance on the desired temperature rise, T_i.

TEMPERATURE RISE WITHIN CONTACT OF ARBITRARY SHAPE

Temperature Rise at Vertex of a Right-Triangle

For the problem illustrated in Fig. 3, the diffusion of heat from a point source qdA into a semi-infinite body or half-space with T = 0 initially and an adiabatic surface, it has been shown that the temperature rise T after some t is given by [2]

$$T = \frac{qdA}{2\pi k\rho}\ \mathrm{erfc}\ \left(\frac{\rho}{2\sqrt{\alpha t}}\right) \qquad (2)$$

where k is the thermal conductivity of the body and α its thermal diffusivity.

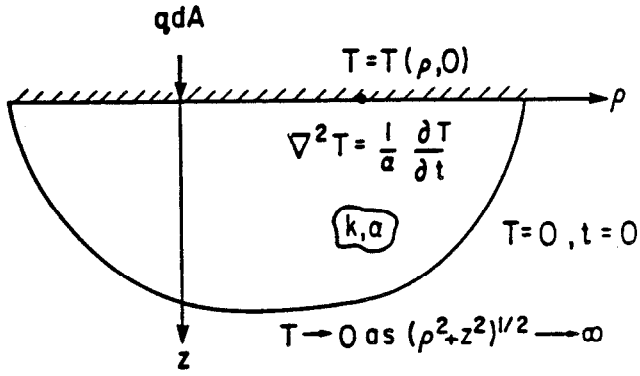

Fig. 3 Point source of heat on adiabatic half-space

If a uniform flux is prescribed over a right-triangular contact area such as Fig. 4, the resulting temperature rise at the vertex is

$$T = \frac{q}{2\pi k}\int_0^{\omega}\int_0^{\delta/\cos\theta}\ \mathrm{erfc}\ \left(\frac{r}{2\sqrt{\alpha t}}\right)\ dr\,d\theta \qquad (3)$$

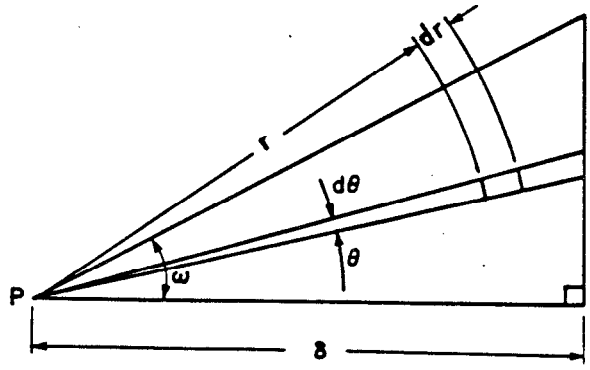

Fig. 4 Integration over right-triangle

Long Time Solution

When t is "large" the argument of the complementary error function becomes small ($r/2\sqrt{\alpha} \ll 1$) and thus the function can be written in a series expansion [3] to give

$$T = \frac{q}{2\pi k}\int_0^{\omega}\int_0^{\delta/\cos\theta}\left\{1 - \frac{2}{\sqrt{\pi}}\left[\frac{r}{2\sqrt{\alpha t}} - \frac{r^3}{24(\alpha t)^{3/2}}\right.\right.$$

$$\left.\left. + \frac{r^5}{320(\alpha t)^{5/2}} - \frac{r^7}{5576(\alpha t)^{7/2}} + \ldots\right]\right\} dr\,d\theta \qquad (4)$$

After evaluating these integrals [4] the temperature rise is

$$T = \frac{q}{2\pi k}\left\{\delta \ln\left[\tan\left(\frac{\pi}{4}+\frac{\omega}{2}\right)\right] - \frac{\delta\tan\omega}{2\sqrt{\pi Fo}} + \frac{\delta\sin\omega}{48\sqrt{\pi}Fo^{3/2}}\left[\left(\frac{2}{3}\sec\omega + \frac{1}{3}\sec^3\omega\right) - \frac{1}{20Fo}\left(\frac{8}{15}\sec\omega + \frac{4}{15}\sec^3\omega + \frac{1}{5}\sec^5\omega\right) + \frac{1}{448Fo^2}\left(\frac{16}{35}\sec\omega + \frac{8}{35}\sec^3\omega + \frac{6}{35}\sec^5\omega + \frac{1}{7}\sec^7\omega\right) - \ldots\right]\right\} \quad (5)$$

where $Fo = \alpha t/\delta^2$ is the Fourier modulus or dimensionless time.

The first term of Eq. (5) is exactly the steady-state result of Yovanovich [5]. The additional terms represent a perturbation from the steady-state result. Note that the error associated with Eq. (5) increases with decreasing time or Fo and with increasing angle ω because the series expansion of the complementary error function becomes invalid over some part of the right-triangle's contact area.

Short Time Solution

If it is assumed that the uniform flux over the right-triangular contact area has been applied only for a relatively short period of time, then it is reasonable to expect that the temperature rise at the vertex will be fairly insensitive to the details of the far boundary of the contact area. Thus for short time only the temperature rise at the vertex of a right-triangle and a sector with the same vertex angle ω and contact area should be approximately identical. By equating the areas of the sector and right-triangle shown in Fig. 5, then

$$a = \delta\sqrt{\frac{\tan\omega}{\omega}} \quad (6)$$

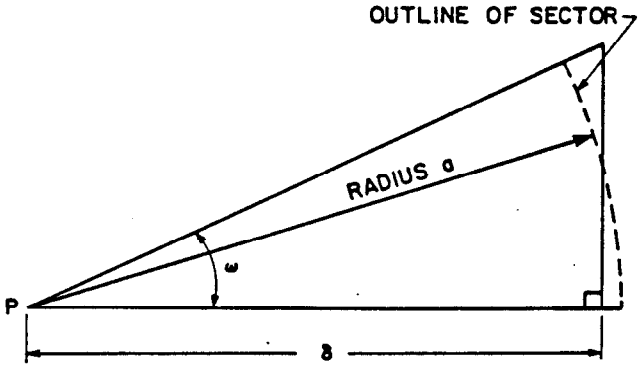

Fig. 5 Approximation of right-triangle by sector of equal area

For the sector the temperature rise at the vertex is given by

$$T = \frac{q}{2\pi k}\int_0^{\omega}\int_0^{a}\operatorname{erfc}\left(\frac{r}{2\sqrt{\alpha t}}\right) dr d\theta \quad (7)$$

These integrations can be evaluated in closed form to give [2]

$$T = \frac{q}{2\pi k}\left\{2\sqrt{Fo'}\,\omega a\left[\frac{1}{\sqrt{\pi}} - \frac{1}{\sqrt{\pi}}\exp\left(\frac{-1}{4Fo'}\right) + \frac{1}{2\sqrt{Fo'}}\operatorname{erfc}\left(\frac{1}{2\sqrt{Fo'}}\right)\right]\right\} \quad (8)$$

where the Fourier modulus Fo' is given by $Fo' = \alpha t/a^2$.

The error associated with using Eq. (8) increases with increasing ω because the shapes of the sector and right-triangle become increasingly different. In addition, the error also increases as Fo' increases since the shape differences noted above contribute more significantly to the temperature rise at the vertex.

Correlation Between Long Time and Short Time Solutions

Equations (5) and (8) give respectively the temperature rise at the vertex of a right-triangle for the long time and short time assumptions. However, some criterion must be developed to determine for any particular angle ω the time t which constitutes the transition from short time to long time. Since both Eqs. (5) and (8) predict temperature rises slightly higher than those obtained by accurate numerical integration, then the transition time or transitional Fourier modulus Fo_{tr} for a particular ω occurs when the two solutions are identical. By investigating particular values of ω in 1-degree intervals from 0° to 85° the following correlations of Fo_{tr} as a function of ω have been made:

$$Fo_{tr} = \frac{1}{4\cos^2\omega}\left\{2.87 - 5.18\omega - 28.2\omega^2 + 95.6\omega^3 - \frac{2.31\times10^{-4}}{\omega}\right\}^2 \quad (9a)$$

for $0° < \omega \le 15°$ ($0 < \omega \le .2618$ rad.), and

$$Fo_{tr} = \frac{1}{4\cos^2\omega}\left\{.944 - .504\omega - .110\omega^2 + .119\omega^3 + \frac{.126}{\omega}\right\}^2 \quad (9b)$$

for $15° < \omega \le 85°$ ($.2618 < \omega \le 1.4835$ rad.) where in both Eqs. (9a) and (9b) the angle ω is in radians and $Fo_{tr} = \alpha t_{tr}/\delta^2$.

For vertex angles of less than 50° the maximum error, which occurs at Fo_{tr}, is about .5%. As the vertex angle ω approaches 75°, maximum error can reach 2-4%. However, it must be noted that the actual error associated with some Fo falls very rapidly to zero as Fo goes above or below Fo_{tr}. In addition, a technique is discussed shortly which virtually eliminates all error for practical applications by making evaluations of the temperature rise by Eq. (5) or (8) with ω large and Fo close to the Fo_{tr} unnecessary.

Superposition of Triangular Elements

Any arbitrary contact geometry can be divided into triangular elements starting from some internal point P at which the temperature rise is to be calculated as shown in Fig. 6. Linear superposition of the temperature rises due to each triangular element can then give an estimate of the temperature rise at P.

Superposition to a General Triangular Element

A triangular element is always orientated as shown in either Fig. 7 or Fig. 8. Each orientation is just a linear combination of two right-triangles which will both have the same Fo.

If the temperature rise at the vertex of a triangular element with vertex angle ω is denoted by $T(\omega)$ then the following summary can be made:

Case 1. From Fig. 7,

$$T(\omega) = T(\omega_1) + T(\omega_2) \quad (10)$$

Case 2. From Fig. 8,

$$T(\omega) = T(\omega_2) + T(\omega_1) \quad (11)$$

where $T(\omega_1)$ and $T(\omega_2)$ are determined by either Eq. (5) or Eq. (8) depending on the long time or short time criterion of Eqs. (9a) and (9b).

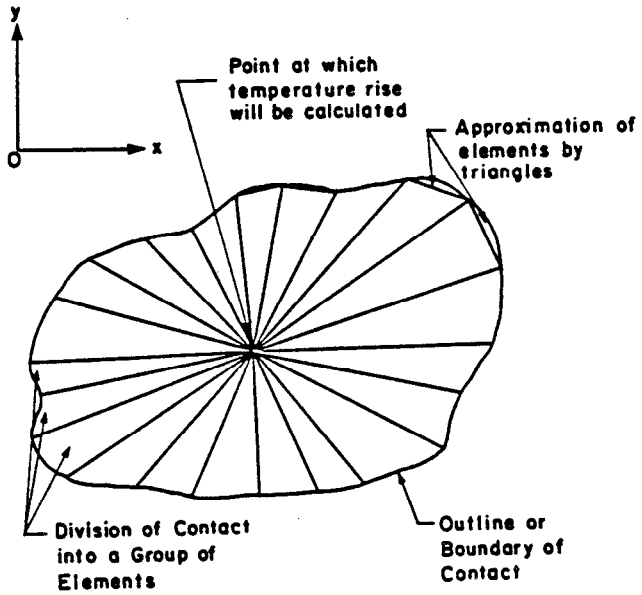

Fig. 6 Discretization of arbitrary contact by triangular elements

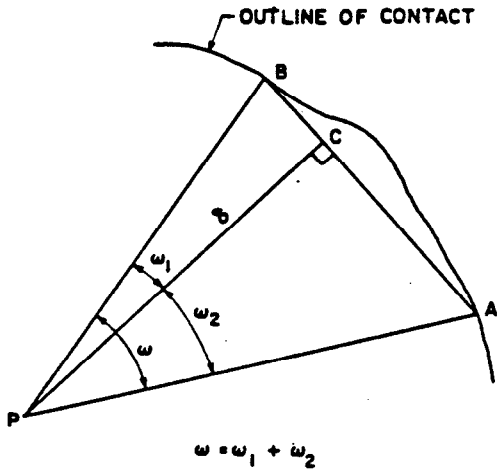

Fig. 7 Division of triangular element into right-triangles (Case 1)

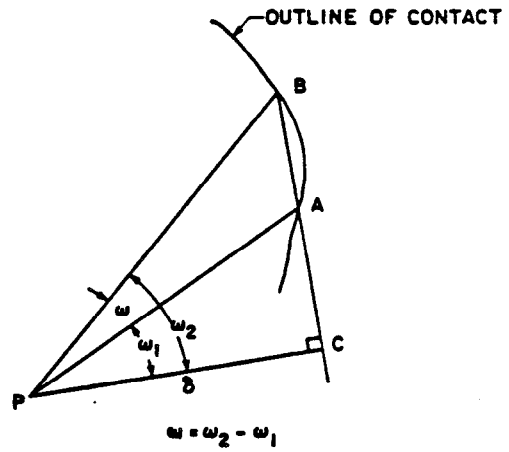

Fig. 8 Division of triangular element into right-triangles (Case 2)

Solution of Thin, Obtuse Triangular Element

In real applications of this method, thin, obtuse triangles as shown in Fig. 9 often arise. Since evaluation of the temperature rise at the vertex of this element involves two right-triangles which both have large vertex angles, substantial errors of 5-10% can arise when the Fourier modulus approaches Fo_{cr} due to subtracting nearly equal numbers each containing some error. To overcome this problem a transformation is made from a thin, obtuse triangular element to a sector element of equal area. If the equal area sector has radius a and the same vertex angle ω then

$$a = \sqrt{\frac{bc \sin \omega}{\omega}} \qquad (12)$$

Equation (8) which was derived from the temperature rise at the vertex of a sector is valid again for this element, or thus

$$T = \frac{q}{2\pi k}\left\{2\omega a \sqrt{Fo'}\left[\frac{1}{\sqrt{\pi}} - \frac{1}{\sqrt{\pi}} \exp\left(\frac{-1}{4Fo'}\right) + \frac{1}{2\sqrt{Fo'}} \operatorname{erfc}\left(\frac{1}{2\sqrt{Fo'}}\right)\right]\right\} \qquad (13)$$

where again $Fo' = \alpha t/a^2$.

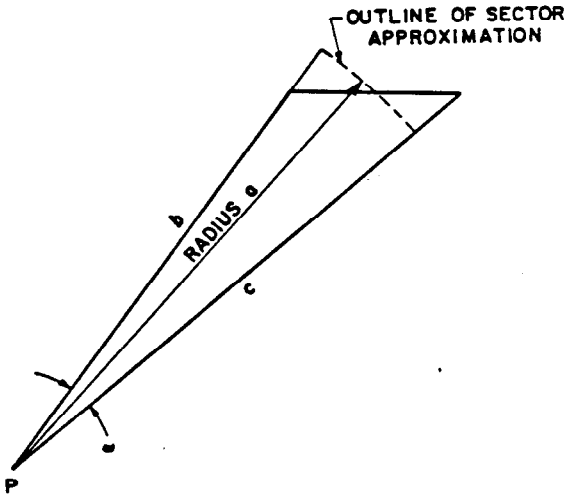

Fig. 9 Sector approximation of obtuse triangular element

This method yields extremely accurate results when Fo approaches Fo_{tr} if the vertex angle ω is kept below 10°. This requirement can always be met by further discretization of the contact shape when necessary. There are two reasons for the success of this technique. First, by keeping the vertex angle small, the differences in the far boundary shape between the sector element and the triangular element are minimal. Second, since this method is used when Fo is near Fo_{tr}, the dimensionless time is still relatively short so the minor differences in shape between the sector and triangular elements do not yet contribute significantly to the temperature rise at the vertex.

Method of Linear Extrapolation

After dividing a contact shape into n elements the total temperature rise at some internal point is simply

$$T_{ii} = \frac{q_i}{2\pi k} \sum_{\ell=1}^{n} T_\ell \tag{14}$$

where T_ℓ represents the temperature rise due to the ℓ^{th} triangular element.

A dimensionless temperature is now introduced by using the square root of the contact area as the fundamental length scale so that,

$$T^*_{ii} = \frac{2\pi k T_{ii}}{q_i \sqrt{A_i}} \tag{15}$$

where A_i represents the total area of the contact. Since the temperature rise is calculated from the sum of triangular element temperature rises, then the total area A_i for non-dimensionalization should be the sum of the areas of the triangular elements

$$A_i = \sum_{\ell=1}^{n} A_\ell \tag{16}$$

where A_ℓ is the area of the ℓ^{th} triangular element.

However, the actual continuous contact shape is approximated by triangles and thus the T* calculated will inherently be somewhat in error even if no errors occurred in the evaluation of each elemental contribution. This occurs because the T* calculated represents a shape with a slightly different boundary and area than the original contact. Thus error in T* arises from area differences lost or gained by the triangular elements.

Figure 10 shows the location of the error causing area A_e. From Fig. 10 it is also apparent that further division of the element will reduce A_e but will still keep A_e at about the same distance from P. Thus, if the error in T* is denoted by ϵ then,

$$\epsilon \propto A_e \tag{17}$$

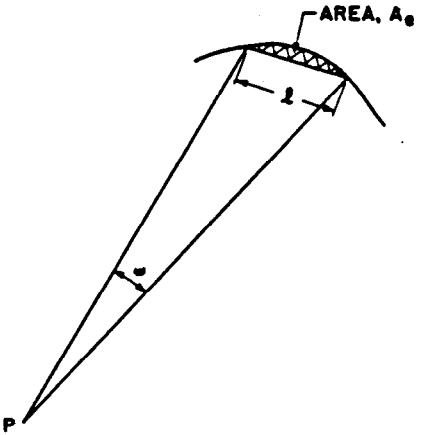

Fig. 10 Area unaccounted by discretization with triangular elements

But if the boundary of the shape is considered circular locally then,

$$A_e \propto L^2 \tag{18}$$

where the chord length L is related to the vertex angle ω such that,

$$L \propto \omega \tag{19}$$

If n equal-angle divisions of the contact shape are made to generate the elements then

$$\omega \propto 1/n \tag{20}$$

And therefore,

$$\epsilon \propto 1/n^2 \tag{21}$$

Thus by plotting values of T* against $1/n^2$, where n is the number of equal-angle elements a linear relationship such as shown in Fig. 11 is obtained. A simple extrapolation of this curve to the intercept where $n = \infty$ gives the T* of the actual contact shape. This technique has been used extensively with great success to generate the data of the next section and in every case a linear plot as shown in Fig. 11 has been observed.

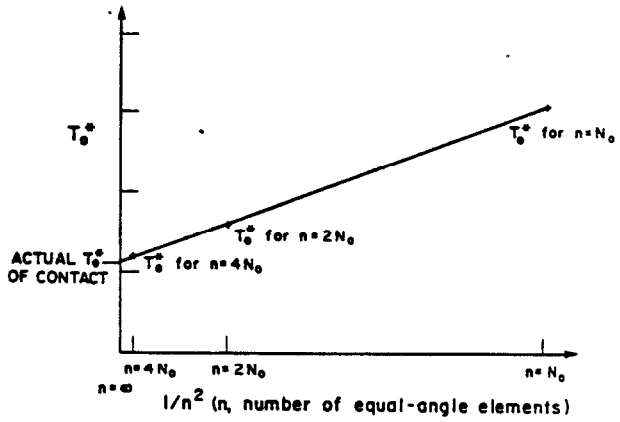

Fig. 11 Extrapolation of computed temperature rises

Results for Several Common Shapes

To illustrate and apply the methods discussed, the dimensionless centroidal temperature rise of an elliptical contact has been calculated over a complete range of dimensionless time Fo^i where

$$Fo^i = \frac{\alpha t}{(\sqrt{A_i})^2} \tag{22}$$

The ellipses are defined by $(x/a)^2 + (y/b)^2 = 1$ where the aspect ratio is b/a. The resultant dimensionless centroidal temperature rises for ellipses of different aspect ratios over the range of 10^{-6} to 10^6 for Fo^i are given in Table 1. Centroidal temperatures are especially important for microelectronics applications since the maximum device temperature is usually located at the centroid of the planar contact.

The analytic solution for the circle is given by Eq. (8) by letting $\omega = 2\pi$. It can thus be shown that the results for the circle in Table 1 are all accurate to the decimal places shown. Note that for all these shapes symmetry was used so that calculations need only be made in the first quadrant. For the circle the necessary initial number of equal-angle elements was $N_o = 2$ (i.e. $2N_o = 4$, $4N_o = 8$). However, as the aspect ratio b/a decreased, the initial number of equal-angle elements increased to $N_o = 4$, $N_o = 8$ and finally $N_o = 16$ for b/a = .1 in order to insure accuracy in every case to the decimal places shown. If less accuracy were required then considerably fewer elements could be used.

$Fo^i \equiv \frac{\alpha t}{(\sqrt{A_i})^2}$	Dimensionless Temperature $T_{ii}^* = \frac{2\pi k T_{ii}}{q_i\sqrt{A_i}}$ at centroid of $\left(\frac{x}{a}\right)^2 + \left(\frac{y}{b}\right)^2 = 1$					
$\log_{10} Fo$	$\frac{b}{a} = 1.0$	$\frac{b}{a} = 0.8$	$\frac{b}{a} = 0.6$	$\frac{b}{a} = 0.4$	$\frac{b}{a} = 0.2$	$\frac{b}{a} = 0.1$
-6	0.0071	0.0071	0.0071	0.0071	0.0071	0.0071
-5	0.0224	0.0224	0.0224	0.0224	0.0224	0.0224
-4	0.0709	0.0709	0.0709	0.0709	0.0709	0.0709
-3	0.2242	0.2242	0.2242	0.2242	0.2242	0.2242
-2	0.7090	0.7090	0.7089	0.7083	0.7001	0.6736
-1	1.9645	1.9574	1.9276	1.8493	1.6494	1.4113
0	2.9881	2.9773	2.9321	2.8137	2.4982	2.1070
1	3.3667	3.3558	3.3098	3.1894	2.8663	2.4601
2	3.4850	3.4775	3.4316	3.3110	2.9876	2.5809
3	3.5271	3.5161	3.4701	3.3496	3.0262	2.6195
4	3.5393	3.5283	3.4823	3.3618	3.0382	2.6317
5	3.5432	3.5322	3.4862	3.3656	3.0422	2.6355
6	3.5446	3.5334	3.4874	3.3669	3.0435	2.6368
∞	3.5449	3.5337	3.4878	3.3678	3.0442	2.6373

Table 1. Dimensionless centroidal temperature rise for ellipses

In Table 2 the dimensionless centroidal temperature rises of five different shapes are tabulated. From these results it is seen that the dimensionless centroidal temperature rise decreases as the contact shape becomes less concentrated about the centroid.

In addition, two major observations can be made from Tables 1 and 2. First by using the square root of area to non-dimensionalize, then the centroidal temperature rise for most shapes up to a Fo^i of 10^{-2} (or up to a Fo^i of 10^{-3} for very narrow shapes) is given simply by

$$T_{ii}^* \approx 4\sqrt{\pi}\,\sqrt{Fo^i} \qquad Fo^i < 10^{-2} \tag{23}$$

which is essentially the analytic solution for uniformly-heated half-space. And second, when the dimensionless time Fo^i reaches 10^2, the centroidal temperature rise of any shape is within about 2% of its steady-state value.

$Fo^i \equiv \frac{\alpha t}{(\sqrt{A_i})^2}$	Dimensionless Temperature $T_{ii}^* = \frac{2\pi k T_{ii}}{q_i\sqrt{A_i}}$ at centroid of various shapes				
$\log_{10} Fo$	Circle	Square	Equilateral Triangle	$\sqrt{\frac{x}{a}} + \sqrt{\frac{y}{a}} = 1$	Semi-circle
-6	0.0071	0.0071	0.0071	0.0071	0.0071
-5	0.0224	0.0224	0.0224	0.0224	0.0224
-4	0.0709	0.0709	0.0709	0.0709	0.0709
-3	0.2242	0.2242	0.2242	0.2242	0.2242
-2	0.7090	0.7090	0.7090	0.7090	0.7087
-1	1.9645	1.9521	1.9151	1.8989	1.8872
0	2.9881	2.9690	2.9111	2.8808	2.8731
1	3.3667	3.3473	3.2883	3.2571	3.2498
2	3.4850	3.4691	3.4100	3.3788	3.3715
3	3.5271	3.5076	3.4486	3.4174	3.4101
4	3.5393	3.5198	3.4608	3.4296	3.4223
5	3.5432	3.5237	3.4646	3.4335	3.4261
6	3.5446	3.5249	3.4659	3.4347	3.4273
∞	3.5449	3.5255	3.4664	3.4356	3.4281

Table 2. Dimensionless centroidal temperature rise for various shapes

TEMPERATURE RISE EXTERIOR TO CONTACT OF ARBITRARY SHAPE

To determine the temperature rise at a surface point exterior to a thermal contact of arbitrary shape, an approximate analysis is developed for both long and short times.

Long Time Solution

If a uniform flux q_j is prescribed on an arbitrary contact area as shown in Fig. 12, then by superposition of the point-source solution [2] the temperature rise at some point P exterior to the contact is

$$T_{ij} = \int_{A_j} \frac{q_j}{2\pi k\rho}\,\mathrm{erfc}\left(\frac{\rho}{2\sqrt{\alpha t}}\right) dA_j \tag{24}$$

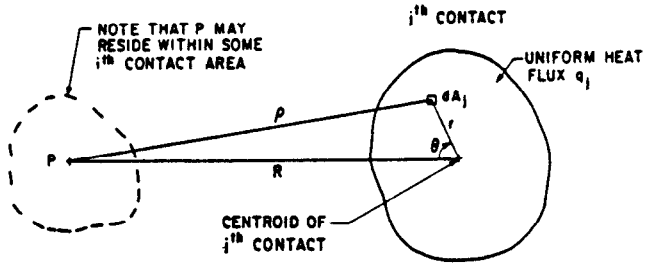

Fig. 12 Integration over arbitrary contact

A series expansion of the complementary error function for large t gives

$$T_{ij} = \frac{q_j}{2\pi k}\left\{\int_{A_j}\frac{dA_j}{\rho} - \frac{1}{\sqrt{\pi}(\alpha t)^{1/2}}\int_{A_j} dA_j + \frac{1}{12\sqrt{\pi}(\alpha t)^{3/2}}\int_{A_j}\rho^2 dA_j - \frac{1}{160\sqrt{\pi}(\alpha t)^{5/2}}\int_{A_j}\rho^4 dA_j + \frac{1}{2688\sqrt{\pi}(\alpha t)^{7/2}}\int_{A_j}\rho^6 dA_j - \ldots\right\} \tag{25}$$

An approximate solution to these integrals can be derived using the methods of [1]. From Fig. 12 application of the cosine law gives

$$\rho^2 = R^2 + r^2 - 2rR\cos\theta \tag{26}$$

where R is the distance from the exterior point P to the centroid of the arbitrary contact shape and (r,θ) represent a local polar coordinate system.

The first integral in Eq. (25) becomes

$$\int_{A_j}\frac{dA_j}{\rho} = \frac{1}{R}\int_{A_j}\left(1 + \frac{r^2}{R^2} - \frac{2r}{R}\cos\theta\right)^{-1/2} dA_j \tag{27}$$

By noting that $r/R < 1$ in general, a binomial expansion of Eq. (27) gives

$$\int_{A_j}\frac{dA_j}{\rho} \approx \frac{1}{R}\left\{\int_{A_j} dA_j + \frac{1}{R}\int_{A_j} r\cos\theta\, dA_j + \frac{1}{2R^2}\int_{A_j}(3r^2\cos^2\theta - r^2)\, dA_j\right\} \tag{28}$$

The first integral is simply

$$\int_{A_j} dA_j = A_j \tag{29}$$

and by definition of the centroidal location

$$\int_{A_j} r\cos\theta\, dA_j = 0 \tag{30}$$

Furthermore,

$$\int_{A_j}(3r^2\cos^2\theta - r^2)\, dA_j = \int_{A_j}(2r^2 - 3r^2\sin^2\theta)\, dA_j = 2I_o - 3I_{RR} \tag{31}$$

where

$$I_o = \int_{A_j} r^2 dA_j \tag{32}$$

$$I_{RR} = \int_{A_j} r^2\sin^2\theta\, dA_j \tag{33}$$

I_o is defined as the polar second moment of area about the centroid of the j^{th} contact and I_{RR} as the radial second moment of area about the axis formed by the exterior point P in Fig. 12 and the centroid of the j^{th} contact. Both quantities are readily available for most common contact shapes such as circles, squares, ellipses and rectangles.

Thus the first integral in Eq. (25) is given approximately by

$$\int_{A_j} \frac{dA_j}{\rho} \approx \frac{A_j}{R} + \frac{2I_o - 3I_{RR}}{2R^3} \tag{34}$$

The second and third integrals in Eq. (25) can be evaluated exactly as

$$\int_{A_j} dA_j = A_j \tag{35}$$

$$\int_{A_j} \rho^2 dA_j = R^2 A_j + I_o \tag{36}$$

By using the same method of variable transformation, binomial expansion and neglecting higher order terms, the fourth and fifth integrals in Eq. (25) can be shown to be

$$\int_{A_j} \rho^2 dA_j \approx R^2 A_j + 2R^2(3I_o - 2I_{RR}) \tag{37}$$

$$\int_{A_j} \rho^6 dA_j \approx R^6 A_j + 3R^4(5I_o - 4I_{RR}) \tag{38}$$

Thus the temperature rise at a surface point P a distance R from the centroid of a thermal contact of arbitrary shape exposed to uniform flux q_j for a "long" period of time is given approximately by

$$T_{ij} \approx \frac{q_j}{2\pi k}\left\{\frac{A_j}{R} + \frac{2I_o - 3I_{RR}}{2R^3} - \frac{1}{\sqrt{\pi}(Fo^j)^{1/2}}\left[\frac{A_j}{R}\right.\right.$$
$$- \frac{1}{12Fo^j}\left(\frac{A_j}{R} + \frac{I_o}{R^3}\right) + \frac{1}{160(Fo^j)^2}\left(\frac{A_j}{R} + \frac{6I_o - 4I_{RR}}{R^3}\right)$$
$$\left.\left. - \frac{1}{2688(Fo^j)^3}\left(\frac{A_j}{R} + \frac{15I_o - 12I_{RR}}{R^3}\right)\right]\right\} \tag{39}$$

where

$$Fo^j = \frac{\alpha t}{R^2} \tag{40}$$

This is referred to as the long time induced-effect temperature rise expression.

Approximate Geometry Solutions (Short Time)

In the preceding section a long time temperature rise expression was developed. Unfortunately, this expression is not valid below $Fo^j \approx .25$ because the series expansion of $\operatorname{erfc}(\rho/2\sqrt{\alpha t})$ diverges. Thus an attempt to determine the induced-effect temperature rise at relatively short times is made by considering two approximate contact geometries which can be solved analytically.

The simplest approximation consists of converting the original problem with a uniform flux over an arbitrary contact area to one with a total heat flux applied as a point-source at the centroid of the contact. With this approximation the temperature rise at a surface point P located a distance R from an arbitrary thermal contact with uniform flux q_j and area A_j as shown in Fig. 12 is simply

$$T_{ij} \approx \frac{q_j A_j}{2\pi k R} \operatorname{erfc}\left(\frac{1}{2\sqrt{Fo^j}}\right) \tag{41}$$

This is referred to as the point-source induced-effect temperature rise expression. This approximation is accurate at all times if the thermal contact is located far enough from the surface point of interest.

A better approximate geometry which can be solved analytically results from transforming an arbitrary contact area to a sector with equivalent area, approximate shape and location. The sector is defined by a local polar coordinate system based at the surface point P as shown in Fig. 13.

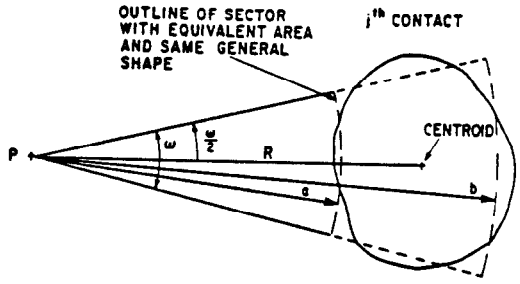

Fig. 13 Sector approximation of arbitrary contact

By approximating the radius of gyration of the sector by that of an equal area rectangle, one can show that with reference to Fig. 13

$$\omega = 2\tan^{-1}\sqrt{3I_{RR}/A_j R^2} \tag{42}$$

For equivalent area and approximate location, then

$$b = R + \frac{A_j}{2\omega R} \tag{43}$$

$$a = R - \frac{A_j}{2\omega R} \tag{44}$$

The resultant temperature rise for the sector approximation can be determined exactly to give

$$T_{ij} \approx \frac{q_j}{\pi^{3/2} k}\left\{\frac{b}{2\sqrt{Fo^b}}\left[1 - \exp\left(\frac{-1}{4Fo^b}\right)\right.\right.$$
$$\left. + \frac{1}{2\sqrt{Fo^b}} \operatorname{erfc}\left(\frac{1}{2\sqrt{Fo^b}}\right)\right]$$
$$\left. - \frac{a}{2\sqrt{Fo^a}}\left[1 - \exp\left(\frac{-1}{4Fo^a}\right) + \frac{1}{2\sqrt{Fo^a}} \operatorname{erfc}\left(\frac{1}{2\sqrt{Fo^a}}\right)\right]\right\} \tag{45}$$

where

$$Fo^b = \frac{\alpha t}{b^2} \tag{46}$$

$$Fo^a = \frac{\alpha t}{a^2} \tag{47}$$

This is referred to as the sector induced-effect temperature rise expression. This approximation is significantly better than the point source at short times and small R since the contact shape is better represented. However at very short time ($Fo^j \ll .1$) and small R, large relative errors in T_{ij} still result since the temperature rise is greatly influenced by the location of the nearest boundary edge of the thermal contact. Note that other criteria could be used to transform an arbitrary shape to an approximately equivalent sector. However the criterion used here results in simple closed-form expressions which reduce to the point-source solution as R becomes very large.

Selection and Accuracy of Solution

A dimensionless distance from the centroid of any arbitrary shape is defined as

$$\beta = R/\sqrt{A_j} \tag{48}$$

To determine a criterion for selecting a solution method, numerical results were generated from all three solution methods over a wide range of Fo^j and β for various common shapes. To make error estimates, accurate results were obtained by numerical integration of the point-source solution. Note that the numerical integration typically consumed 1000-10,000 times the computation of the three approximate analytical solutions for 1% or better convergence of results. The criteria for selection of a solution method is summarized graphically in Fig. 14.

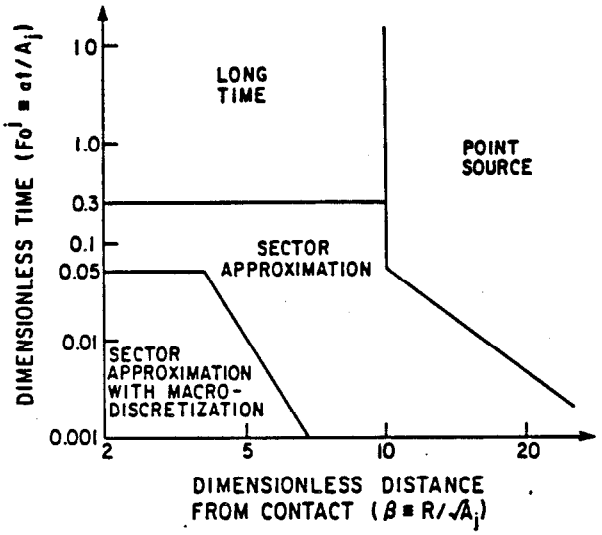

Fig. 14 Solution method selection criteria

From the extensive results compiled, when β becomes large ($\beta > 10$), then simple point-source induced-effect temperature rise expression of Eq. (41) is adequate except when Fo^j is very small ($Fo^j \ll .1$). The long time induced-effect temperature rise expression of Eq. (39) works well for any β on most common shapes when $Fo^j \geq .3$. When $Fo^j \leq .3$ and $\beta < 10$, the sector induced-effect temperature rise expression of Eq. (45) becomes the proper solution method.

Unfortunately even the sector approximation works poorly sometimes when Fo^j is on the order of 0.1 or less and β is relatively small ($\beta \leq 3$ - 5). When such cases arise, macro-discretization of the contact shape (e.g. sub-divide a square contact into 4 or 9 smaller square areas) is required since the β associated with each smaller contact area is larger. The solution is then found by superposing the individual temperature rises for each discretized contact area. However in most engineering applications this situation is unimportant since even at $\beta \approx 2$ and $Fo^j \approx .01$ the resultant T_{ij} is usually about 10^{-5} of its steady-state value and is much smaller than any T_{ii} for a point P within interior to another contact, or essentially zero.

From the results compiled for several common shapes under different orientations, some cautious generalizations can be made relating errors to the solution method at various values of β and Fo^j. When β is small ($\beta \approx 2$) and $Fo^j \approx .3$, the long time solution method was typically 1% or less in error. This difference diminishes rapidly as β and Fo^j increased. Errors of 10% or less were usually observed for small β ($\beta \leq 5$) and $.05 \leq Fo^j \leq .3$ when using the sector approximation. Thus, if extreme accuracy is desired, macro-discretization may be necessary for any $Fo^j \leq .3$ and $\beta \leq 5$, or for any Fo^j when $\beta \leq 2$. However, such situations are either rare or unimportant in most applications envisioned for this method.

APPLICATION TO SYSTEMS OF ARBITRARILY SHAPED CONTACTS

For a system of arbitrary planar contacts on a half-space as shown in Figs. 1 and 2, the temperature rise at some point within the i^{th} contact area was written in Eq. (1) as a linear superposition of the temperature rises due to each contact in the system. When the heat flux over each contact area in the system is modelled as uniform and the surface region between the contacts adiabatic, then the methods developed in this work can be used to evaluate the T_{ii} and T_{ij} for a given time. Furthermore, Eq. (1) can also be written as a system of linear equations in the matrix form

$$[G_{ij}](q_j) = (T_i) \tag{49}$$

where the entries in the matrix $[G_{ij}]$ are functions of the geometry and placement of the contacts, the thermal properties and the elapsed time of the thermal loading. This matrix formulation of Eq. (49) allows more general problems for a system of arbitrary contacts under transient conditions to be considered. For example, if in a particular application some maximum temperature rises are specified for the contacts after some period of time, then the corresponding maximum tolerable heat fluxes q_j on the contacts can be calculated simply by solving the linear equations posed by Eq. (49).

Often the quantity of interest is not the actual temperature versus time history for a system, but simply the time required to reach say 95% or 99% of the steady-state temperature rises. This type of problem can be handled by examining the T_i predicted by Eq. (49) at various times t with the T_i for steady-state results. Note that the steady-state results can be obtained by letting $t \to \infty$ in all of the expressions derived in this work.

Another possible application is the determination of the average temperature or thermal resistance of a single contact or arbitrary shape on an adiabatic half-space under transient conditions. This can be accomplished by using a method outlined in [1]. In that paper it was shown that the thermal resistance or average temperature of a uniformly distributed system of circular contacts is typically only 5% higher than that of a shape which outlines the system of contacts when the total area of the contacts is about 20% of the area of the shape. By combining the expression for T_{ii} and T_{ij} (i.e. evaluate $[G_{ij}]$) developed in this work with the extrapolation techniques of [1], the thermal resistance or average temperature rise of any arbitrarily shaped contact on an adiabatic half-space can be determined under transient conditions for any contact boundary condition.

Finally, it has been implicitly assumed throughout the derivations of this work that all the contacts begin heating at the same time $t = 0$ into a uniform temperature half-space. Although this is required mathematically, results can still be obtained when the contacts begin heating at different times at least to some first approximation. This is possible because even under steady-state conditions the temperature field surrounding a contact on a half-space is nearly uniform everywhere except for a small constriction zone in the immediate vicinity of the contact. Under transient conditions this contact constriction zone becomes even smaller. Thus at some time $t_i = 0$ when thermal loading begins on the i^{th} contact, the temperature rise near this contact is always somewhat uniform, although not necessarily zero, provided the contact is not located very close to another contact which has been thermally loaded for long periods of time.

CONCLUSIONS

Approximate methods to determine the temperature rise under transient conditions at surface points interior and exterior to arbitrarily-shaped contacts with uniform flux on a half-space have been developed.

For the interior problem, an arbitrary contact shape is divided into macro-surface elements triangular in shape with a common vertex at the point at which the temperature rise is required. An approximate analysis is then used to

evaluate the temperature rise contribution of each triangular element for any given time of thermal loading. By means of a method of extrapolation, accurate results can be obtained with relatively few macro-surface elements.

Separate methods have also been developed to predict the transient temperature rise at points exterior to the contacts for both short and long dimensionless times of thermal loading. Although the simple expressions developed are found by integrating over the entire arbitrary contact shape, in some special cases macroscopic sub-division of the contact shape must be made.

The resultant approximate expression for the self-effect and induced-effect components are easily implemented on a microcomputer. With the concept of linear superposition, a system of algebraic equations is formulated to relate the contact fluxes and temperatures to the elapsed time of thermal loading, the contact geometry, and the thermal properties. The computational efficiency of the approach allows predictions of the transient thermal behaviour of large systems of planar contacts to be made rapidly on a microcomputer.

ACKNOWLEDGEMENTS

The authors thank Dr. J.C. Thompson of the Department of Civil Engineering at the University of Waterloo for his comments and suggestions. The authors also acknowledge the financial support of the Natural Sciences and Engineering Research Council of Canada under operating grant A7455 for Dr. Yovanovich and from a Postgraduate Scholarship for Mr. Negus.

REFERENCES

[1] Yovanovich, M.M., Thompson,J.C. and Negus, K.J., "Thermal Resistance of Arbitrarily Shaped Contacts", Third International Conference on Numerical Methods in Thermal Problems, Seattle, WA, Aug. 2-5, 1983.

[2] Carslaw, H.S. and Jaeger, J.C., *Conduction of Heat in Solids*, Oxford University Press, London, 1959.

[3] Abramowitz, M. and Stegun, I., *Handbook of Mathematical Functions*, Dover Publications, New York, 1971.

[4] Gradshteyn, I.S. and Ryzhik, I.M., *Tables of Integrals Series and Products*, Academic Press, New York, 1961.

[5] Yovanovich, M.M., "Thermal Constriction Resistance of Contacts on a Half-Space: Integral Formulation", AIAA Paper 75-708, AIAA 10th Thermophysics Conference, Denver, CO, May 27-29, 1975.